Simultaneous Determination of Horizontal and Vertical Accuracy of ICESat-2 in McMurdo Dry Valleys, Antarctica

Beata Csatho[1],Tony Schenk[1],Tom Neumann[2]

[1] Dept. of Geology, University at Buffalo, Buffalo,NY, 14260, USA - bcsatho@@buffalo.edu, afschenk@buffalo.edu
[2]NASA Goddard Space Flight Center, Greenbelt MD - thomas.neumann@nasa.gov

Keywords: ICESat-2, laser altimetry, ice sheet mass balance, validation, Antarctica, DEMs

Abstract

This contribution presents an assessment of the horizontal and vertical accuracy of altimetry observations collected by NASA’s Ice, Cloud, and Land Elevation Satellite-2 (ICESat-2) mission. We selected the terrain-matching method to determine the position of laser altimeter profiles within a precisely known surface, represented by a digital elevation model (DEM). We took this classical approach a step further, approximated the DEM by planar surface patches, and calculated the optimal position of the laser profile by minimizing the square sum of the elevation differences between reference DEMs and ICESat-2 profiles. We found the highly accurate DEMs of the McMurdo Dry Valleys (DV), Antarctica, ideal for this research because of their stable landscape and rugged topography. Here, we summarize recent improvements of this approach to estimate the horizontal and vertical accuracy of ICESat-2 observations and assess the quality of new ICESat-2 data releases.

1. Introduction

NASA’s Ice, Cloud and land Elevation Satellite-2 (ICESat-2) satellite, launched in 2018, carries the Advanced Topographic Laser Altimeter System (ATLAS), the first photon-counting laser altimeter orbiting the Earth. ICESat-2 provides observations of essential climate variables of the cryosphere, biosphere, hydrosphere, and atmosphere (Magruder et al., 2024).

By monitoring ice-sheet and glacier elevations, the ATLAS observations enable the estimation of ice-sheet mass balance and thus land ice contributions to sea level rise. Considering the vast extent of the Antarctic ice sheets makes it clear that small height changes may have a considerable impact on the mass balance and corresponding sea level rise estimates. Therefore, ICESat-2 has very stringent accuracy requirements,” *ICESat-2 shall produce an ice surface elevation product that enables determination of ice-sheet elevation change rates to an accuracy of better than or equal to 0.4 cm/yr on an annual basis*” (Markus et al., 2017).

Achieving the centimeter-level accuracy to fulfill the mission’s goals requires high geolocation accuracy and poses a challenge for mission design and operations. For example, changes in sun-orbit geometry induce thermal-mechanical stress, causing a time-varying misalignment. Determining and correcting such minor and constantly changing system deformations requires highly specialized know-how and sophisticated calibration procedures. The calibration identifies errors and corrects them. On the other hand, validation is only concerned with quantifying errors.

We have been engaged in ICESat-2 calibration/validation (Cal-Val) activities and introduced a new methodology for defining differences between highly accurate surfaces and ATL03 laser data. We modified the traditional laser scanning calibration/validation approach to work with natural surfaces (e.g., DEMs) by estimating mathematical functions to find the closest distance between a laser profile and the analytical function. This novel approach offers the calculation of the 3D translation vector and provides rigorous information about error quantities related to the unknowns (Schenk et al., 2022).

2. Background

ATLAS is the laser altimetry system of ICESat-2. The single photon counting instrument produces one laser pulse, which is split into six beams. Each laser beam illuminates a spot on the ground that has a diameter of about 11 m. As Figure 1 shows only a minuscule amount of photons make it to the ground (photon P2 and P4) but only P2 is actually recorded at the telescope. Photon P1 is also recorded but it is reflected from particles in the atmosphere. Same holds for photon P5 however it does not originate from the transmitter. P3 is reflected from within the atmosphere and never made it back to the telescope. One should keep in my that ATLAS is constantly recording photons from these different origins and therefore, identifying the surface from the photon cloud is a challanging problem.

The six beams of ATLAS are mounted on a plate that is slightly rotated about the vertical z-axis. It causes the forward and backward beams in each beam pair to shift on the ground by ~ 90 m reelative to each other. To facilitate different applications, NASA processes the ATLAS altimetry observations into different products that are available through the National Snow and Ice Data Center (NSIDC). The ATL03 Geolocated Photon Data are provided in a geodetic reference frame. In ATL03, the signal photons are identified and various geophysical corrections are applied on the photon height (Neumann et al., 2019). The ATL06 Land Ice Elevation Surface height is derived from ATL03 (Smith et al., 2019) to estimate ice sheet surface elevations along Ground Tracks (GT), spaced every 20 m. ATL06 includes additional corrections to make it suitable for ice sheet studies, for example it is corrected to the first photon bias that causes height errors on highly reflective surfaces. However, since it is derived using a planar fitting algorithm, ATL06 is not depicting the details of rugged topography well. Most of

the results in the paper is derived from ATL03 data because of its superior performance for calibration/validation.

3. Review of Methodology

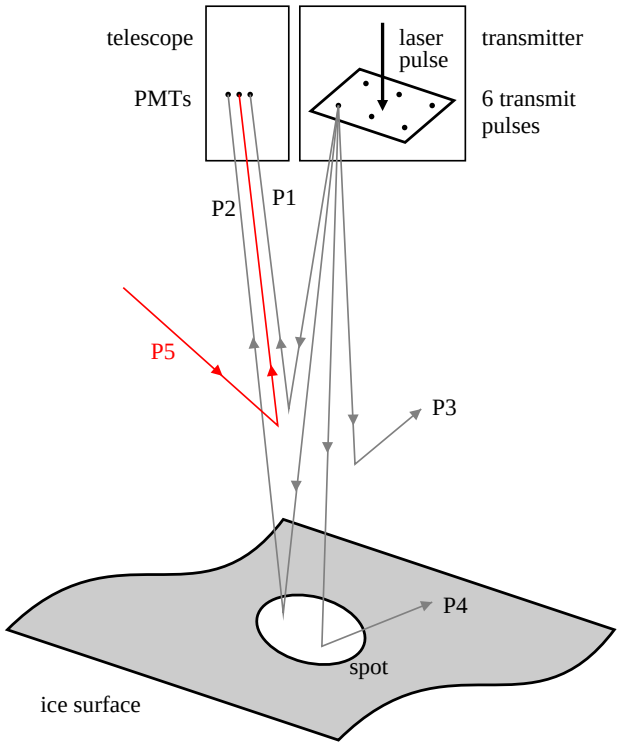

Figure 1. Sketch of photon-counting system principles.

This paper reports about several significant improvements since our last publication (Schenk et al., 2022)

A popular method to determine the difference between a laser altimeter profile and a natural surface is the terrain-matching approach. Here, the laser profile is shifted within a DEM, and the position of the 3D shift is recorded. After all the shifting positions within the search window are known, the position with the shortest distance is considered the best match between the laser profile and DEM. We have improved this approach by replacing the DEM with an analytical surface. This allows us to compute the shortest distance between the laser profile and DEM, casting the terrain-matching problem as a least-squares solution.

$$d = x\cos\alpha + y\cos\beta + z\cos\gamma \tag{1}$$

Eq. 1 displays the shortest distance, d, from a point to a plane, represented by the three directional angles α, β, γ (angles between the coordinate axes and the the normal vector of the plane); ρ is the distance from the origin of the coordinate system perpendicular to the plane. Now we introduce an unknown translation vector, $(t = \Delta x, \Delta y, \Delta z)$ (shift parameter) and formulate the following 3D observation equation:

$$res = (x+\Delta x)\cos\alpha + (y+\Delta y)\cos\beta + (z+\Delta z)\cos)\gamma - \rho \tag{2}$$

The residual, res, is on the left side of the equation. It is the difference between the original observation and the estimated value from the adjustment.

The implementation of the model occurs in several steps. It begins with determining the correspondence between laser ground tracks and DEMs. The datasets are examined on this occasion, mainly to eliminate gross blunders and assess if the data is suitable. The next step is considered with checking the laser profile. Under suitable circumstances, a laser beam may contain about 14 photons in the neighborhood of the surface, and the weak beam has one-fourth of the signal photons. If more than one photon per beam is available the average of all the photons is computed and used in later steps.

The next step is concerned with computing planes along the ground track of one beam (Figure 2). The planes are bounded, and the size is determined by the grid spacing of the DEM and the number of points contributing to the plane. We have chosen a 50 m by 50 m size for the plane. Considering 1 m grid spacing, we have, in theory, 2500 DEM grid points. The large redundancy makes it easier to reject planes having too rough a topography.

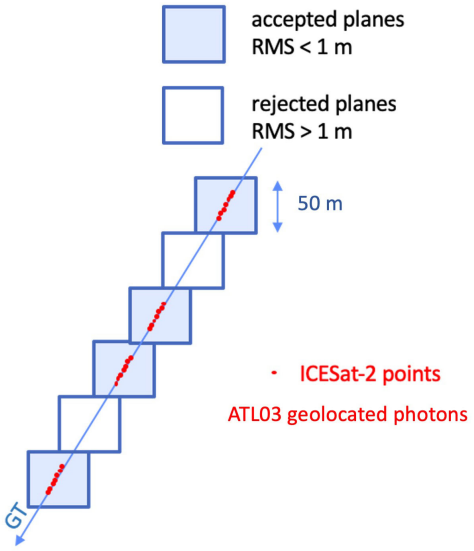

Figure 2. Defining the planes along an ICESat-2 Ground Track.

After selecting suitable planes, we are ready for the adjustment phase. The net result is the translation vectors (shifts) for every beam (Figure 3). The last step is collecting and storing the main adjustment results, including the transformation of the 3D coordinate system to an along/across track system for more convenient comparisons with other studies.

The adjustment model has several advantages. The least-squares adjustment offers the possibility of computing the variance-covariance matrix for a rigorous error assessment. The inverse of the normal equation matrix contains in its diagonal the standard deviations, σ, of the unknown translation vectors. Off-diagonal elements are the correlation coefficients. Another distinct advantage is the flexibility of the mathematical model. We currently use the straightforward model of the translation vector as unknown parameters, but nothing would hinder us from introducing more parameters. An example would be adding a rotation about the z-axis or the simultaneous adjustment of all six beams of a ground track.

The processing of ATL03 photon heights is illustrated in Figure 4. Blue dots are marking signal photons, which are averaged

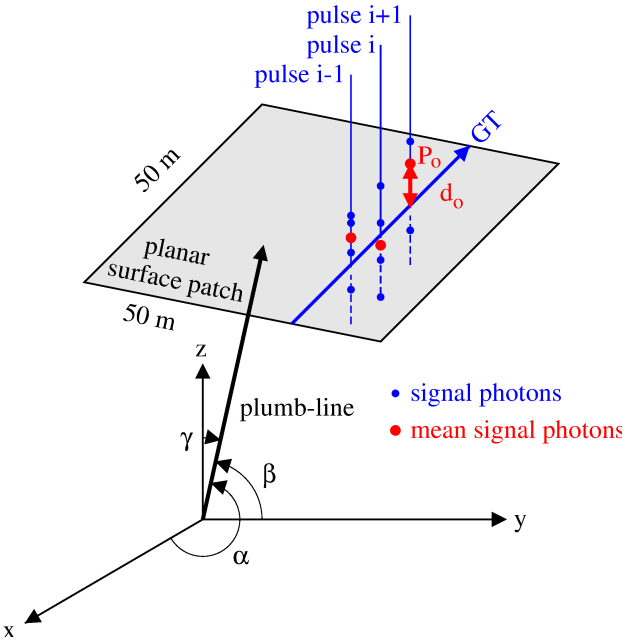

Figure 3. Schematic of determining translation between 3D point data sets using linear approximation of natural surfaces through adjustment (from Schenk et al., 2022).

in each ATLAS footprint to obtain the estimated surface elevation in each laser pulse (ASPEPP). Red dots mark the footprint elevations on planar surface patches that are used in the adjustment, while those in purple lie on rugged surfaces and not used. As seen in the enlargement, the adjustment moves the ATL03 photons to a new location where they agree well with the reference DEM.

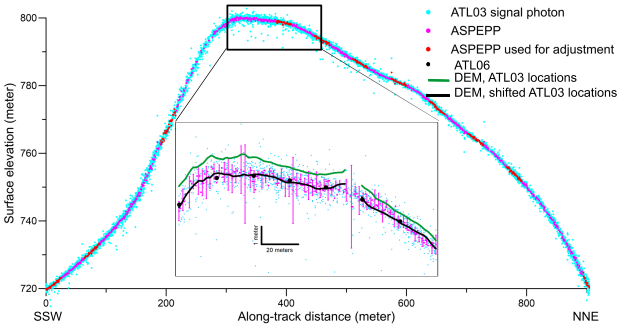

Figure 4. Illustration of method using a ATL03/ATL06 profile from the McMurdo Dry Valleys (see Figure 5 for location).

4. Results

4.1 McMurdo Dry Valleys, East Antarctica, an ideal validation site for ICESat-2

Applying our methodology requires a well-surveyed, stable terrain, preferably free of vegetation and seasonal snow cover. A suitable terrain was found in the Antarctic Dry Valleys (Figures 5 and 6). We selected ICESat-2 repeat ground tracks (RGT) 275 and 451 for the ICESat-2 accuracy assessment (Figure 5) as they provide the most comprehensive coverage over stable terrain away from the coast where surface degradation intensified in recent years (Fountain et al., 2014).

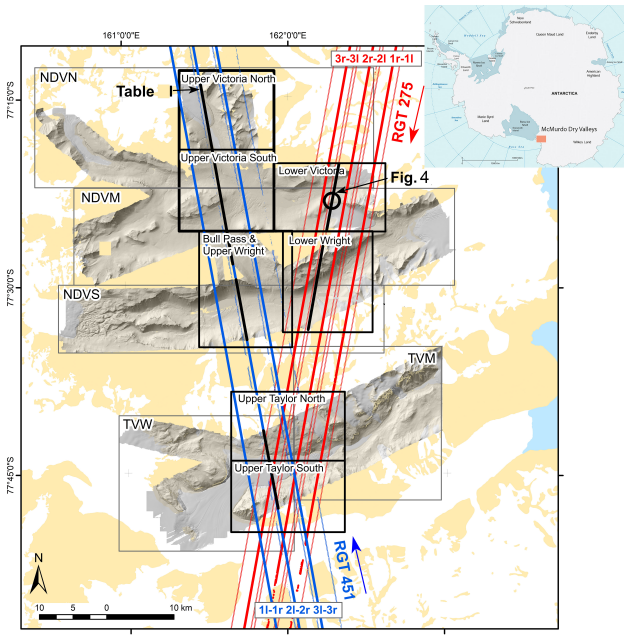

Figure 5. Map showing shaded relief NCALM DEMs used in the study. RGT 275 and RGT 451 are red and blue lines (cycles 1-2, thin lines, cycles 3-14, thick lines). Yellow regions mark rock outcrops, white shoes ice sheet and outlet glaciers and blue is Ross Sea (from Antarctic Digital Database, 2000).

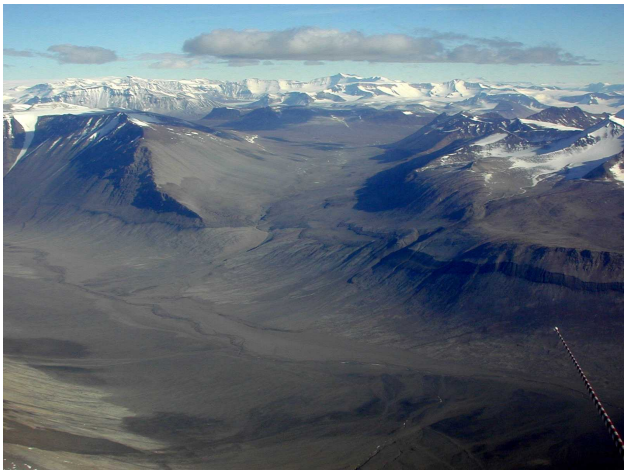

Figure 6. McMurdo Dry Valleys, West Antarctica. Aerial view toward Bull Pass from Wright Valley. Photograph from Jash Landis, NSF, US Antarctic Program Photo Library.

The McMurdo Dry Valleys is a polar desert with a rugged topography, characterized by flat valleys and steep slopes of solid rock outcrops. There is negligible precipitation with erosion limited to the coastal region.

The area has been surveyed twice with airborne laser altimetry to study the magnitude and spatial distribution of landscape changes with increasing climate warming.

The first survey used NASA’s Airborne Topographic Mapper (ATM) system during the austral summer of 2001-02 (Csatho et al., 2005).

A repeat survey was performed by the National Center for Airborne Laser Mapping (NCALM) in 2014-2015 using a Titan

multiwave airborne laser system that collected laser measurements with 5 returns per square meter density (Fountain et al., 2017). The survey covered more than 3,500 km^2 of the Dry Valleys, focusing on the valley floors and neighboring hillslopes. A vertical accuracy of $\pm$ 0.07 m was reported and a 1 meter-resolution DEM was generated for the entire survey area (Figure 5).

4.2 Estimating the 3D translation vector between the reference surface and the ATLAS ATL03 observations

We assessed the error of ICESat-2 by calculating the translation vectors between ICESat-2 observations and the NCALM reference DEM in the Dry Valleys validation site. The validation site was divided into smaller DEMs (Figure 5, e.g., Upper Victoria North, UVN). We obtained 3D translation vectors by computing the shortest distance between GT segments and the precise DEMs using the adjustment solution described in Section 3 for each ICESat-2 data acquisition along the selected GTs; each GT/DEM combination provided one translation vector estimate (Table 1).

	Translation vectors			DEM		accuracy		
B	AL [m]	AC [m]	V [m]	name	length [km]	σ_{AL} [m]	σ_{AC} [m]	σ_{V} [m]
3	1.45	-1.71	0.06	UVN	11.1	0.04	0.07	0.01
	0.72	-1.86	0.10	UVS	12.4	0.04	0.03	0.01
	1.27	-2.02	-0.10	BP	16.3	0.06	0.02	0.01
	0.90	-3.45	0.03	UTN	4.1	0.13	0.09	0.02
	0.82	-1.42	0.33	UTS	7.2	0.08	0.04	0.01
4	-1.14	-2.33	0.08	UVN	11.1	0.06	0.09	0.01
	-2.84	-1.94	0.15	UVS	12.4	0.07	0.06	0.01
	-2.61	-1.87	-0.07	BP	16.3	0.08	0.04	0.01
	-2.93	-1.89	0.19	UTN	4.1	0.30	0.12	0.02
	-3.16	-0.88	0.26	UTS	7.2	0.09	0.05	0.01

Table 1. Translation vectors and their errors calculated for the central beam pair 3 and 4, RGT 451, cycle 3, April 27, 2019; ATL03, Release 5. B: beam number; AL: along-track, AC: across-track, V: vertical components of translation vector. DEMs involved: UVN = Upper Victoria North, UVS = Upper Victoria South, BP = Bull Pass & Upper Wright, UTN = Upper Taylor North, UTS = Upper Taylor South (see Figure 5 for locations of GTs and DEMs).

Although the translation vectors were always calculated with a 3D model, as our research first focused on assessing ICESat-2's horizontal accuracy, we only reported the horizontal translation vector estimates in (Schenk et al., 2022). Here, we also analyze the vertical component of the translation vectors to assess the vertical error of ICESat-2 observations (Table 1).

Table 1 shows results along a single ICESat-2 ground track (RGT 451, cycle 3, April 27, 2019, Release 5) from beams 3 and 4. The accuracy of the translation vectors is provided by the least-squares adjustment. Translation vectors are computed for each NCALM DEM separately to assess the temporal variation of the ICESat-2 horizontal and vertical errors. All components of the translation vector shows significant differences over the different DEMs, indicating that high-frequency, jitter variations have an impact on the geolocation of ICESat-2 photons as discussed in Section IV.C of (Schenk et al., 2022).

4.3 Repeating horizontal error assessment for new releases

During the first two years of the ICESat-2 mission (cycles 1-9), we computed the 3D translation vectors for 379 laser altimeter profiles along the two reference ground tracks. Analyzing these results revealed a total geolocation error(mean + one σ) of 4.93 m for ICESat-2 release 3 and 4.66 m for release 4, well within the mission requirement of 6.5 m (Schenk et al., 2022).

We used the same profiles to compare the accuracy of the release 4 and 5 ATL03 products. The very small difference between the results for these releases (Table 2) indicates a stable, robust and accurate calibration performance (Luthcke et al., 2021).

Since the topography of the McMurdo Dry Valleys is stable, the site is suitable for continuously validating ATLAS and ICESat-2 accuracy without the need of additional *in situ* observations or remote sensing surveys. Therefore, as the mission progressed, we extended the temporal coverage of our analysis by adding ATL03 observations from ICESat-2 cycles 10-14 to obtain more than 600 translation vectors for the period between October 2018 - March 2022 (cycle 1-14). As shown in Table 2, ICESat-2' horizontal accuracy remained remarkably stable.

B	Rel004, cycle 1-9			Rel005, cycle 1-9			Rel005, cycle 1-14		
	N	Hor [m]	σ_{Hor} [m]	N	Hor [m]	σ_{Hor} [m]	N	Hor [m]	σ_{Hor} [m]
1	64	3.12	2.12	64	3.43	2.11	95	3.42	1.91
2	61	2.82	1.71	65	2.99	1.47	97	3.07	1.43
3	72	2.84	1.47	73	2.90	1.32	104	3.24	1.38
4	69	3.06	1.78	73	3.25	1.69	104	3.35	1.71
5	70	2.37	1.23	71	2.52	1.13	102	2.85	1.51
6	61	3.13	2.12	67	3.30	1.82	94	3.51	1.93

Table 2. Horizontal error of the six ICESat-2 beams, release 4 and 5. Column Hor is the horizontal error estimated as the mean of the horizontal component of N translation vectors. The parameter σ_{Hor} refers to the uncertainty of the horizontal error. All units are in meter.

4.4 Assessing the vertical error of iCESat-2

NASA established a precisely surveyed 750 km traverse along the southern latitudinal boundary of ICESat-2 (88^{o}S) in Antarctica to validate the accuracy of photon-based heights and segments of ATL03 and ATL06 (Brunt et al., 2019). The traverse was planned to be surveyed periodically during the lifetime of ICESat-2 using ground-based Global Navigation Satellite Systems (GNSS) and Global Positioning System (GPS). However, after several successful seasons (e.g., Brunt et al., 2019), recent large precipitation events prevented the survey of the (88^{o}S) traverse during the 2023-24 austral summer and further surveys are not logistically feasible.

The Dry Valleys provides an alternative, although much smaller validation site compared to the 750 km ice sheet traverse. However, it is suitable for continuous assessment of the ICESat-2

height error. To test our methodology, we estimated the error by calculating the vertical component of the translation vector using all observations along RGTs 275 and 451 between October 16, 2018 and January 20, 2022 (Table 3). Note that translation vectors were calculated for each DEM (as labeled in Figure 5) and each date of ICESat-2 data acquisition, resulting approximately 100 estimates of vertical accuracy for each beam (see column N in Table 3).

Beam	N	Vertical error [cm]	$\sigma_{\text{VerticalError}}$ [cm]	$stdev_{\text{VerticalError}}$ [cm]
1	99	6.17	0.24	14.05
2	101	3.78	0.98	15.70
3	106	7.36	0.60	13.50
4	106	7.19	0.42	13.7
5	107	3.48	0.52	18.53
6	100	5.89	0.70	17.26

Table 3. Vertical errors of the six ICESat-2 beams, ATL03 product, release 5. Column Beam is laser beam number, N is the number of translation vectors calculated, Vertical error is the estimated vertical error in cm. The parameter $\sigma_{\text{VerticalError}}$ refers to the uncertainty of the vertical error and $stdev_{\text{VerticalError}}$ is the standard deviation of the vertical error. ICESat-2 observations along RGT 275 and 451, between October 16, 2018 – January 20, 2022.

Our ICESat-2 height error estimates are all positive, i.e., ICESat-2 is above the reference DEM, and similar for all beams. They show good agreement with previous estimates from the 88^{o}S traverse obtained from release 1 (Brunt et al., 2019) and release 5 (Luthcke and Brunt, 2023).

4.5 Identifying new validation sites

Another objective of our research is identifying new validation sites to assess ICESat-2 performance around the globe and compare the results with those obtained in the McMurdo Dry Valleys. This is especially important in the northern hemisphere, where only limited assessments have been performed.

In order to detect systematic differences in the translation vectors at different geographic locations it is of paramount interest to perform our analysis at such locations. Suitable locations in the Arctic include outcrop regions along the coastline of Greenland that are surveyed with high-accuracy airborne altimetry neasurements. For example, in Devon Island, NASA’s ATM system underflown the left and right beam pairs of several RGTs, on April 3, 2019 simultaneously with ICESat-2 data acquisition. Another area with a similar constellation is Disko Island, West Greenland, where on May 15, 2019 ATM underflown the left and right beam pairs of several RGTs (Figure 7).

Over the past decade, there has been dramatic growth in the acquisition of high-resolution topographic data for research purposes, which are now available, for example, through OpenTopography (https://opentopography.org/). Several surveyed region s appear to have the characteristics suitable for assessing the accuracy of ICESat-2, such as a rugged surface with surface normals pointing in different direction, stable ground, and no vegetation. A particularly promising site is the Mojave Desert,

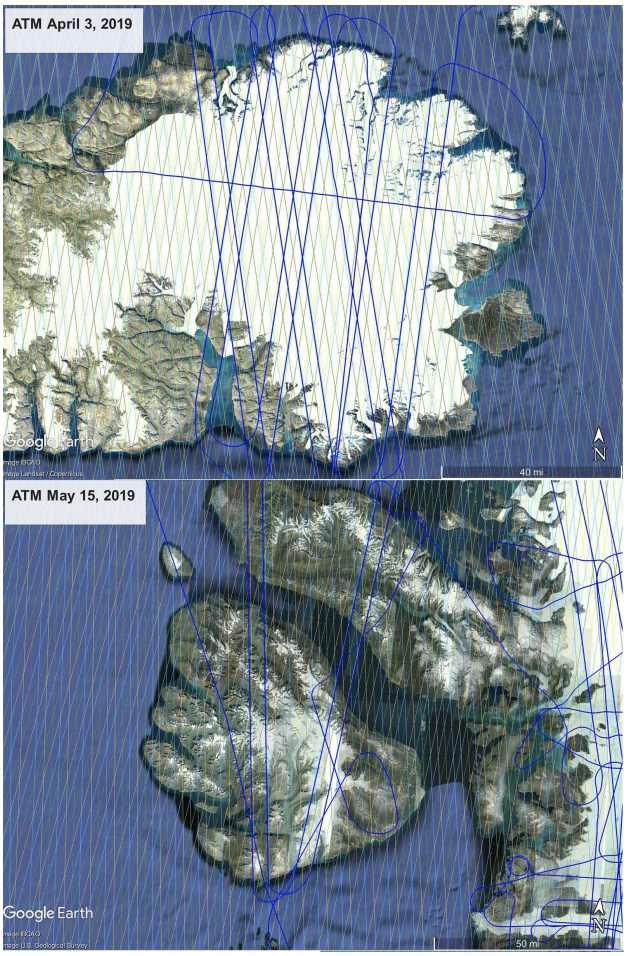

Figure 7. Maps of Devon and Disko Islands in the Arctic showing ICESat-2 groundtrack and ATM flight trajectories.

which was earlier identified as a suitable calibration site for ICESat, NASA’s previous satellite mission, operated between 2003-2009 (Zwally et al., 2002).

5. Conclusions

Our validation approach is unique as it provides a snapshot of the biases with an accuracy assessment without the need of installing special instrument or targets (e.g. corner reflectors)l in the field. Moreover, we assessed the accuracy near the Antarctic ice sheet, the most important target of the ICESat-2 mission. We will continue monitoring the ATLAS performance using the Dry Valley site, employing modified and improved sensor models and extend our validation activity to additional sites.

References

Brunt, K. M., Neumann, T., Smith, B. E., 2019. Assessment of ICESat-2 Ice Sheet Surface Heights, Based on Comparisons Over the Interior of the Antarctic Ice Sheet. *Geophysical Research Letters*, 13(2), 615 – 7.

Csatho, B., Schenk, T., Krabill, W., Eos, T. W., Transactions, 2005, 2005. Airborne laser scanning for high-resolution mapping of Antarctica. *Eos Trans. AGU*, 86(25).

Fountain, A. G., Fernandez-Diaz, J. C., Obryk, M., Levy, J., Gooseff, M., Horn, D. J. V., Morin, P., Shrestha, R., 2017.

High-resolution elevation mapping of the McMurdo Dry Valleys, Antarctica, and surrounding regions. *Earth System Science Data*, 9, 435 – 443.

Fountain, A. G., Levy, J. S., Gooseff, M. N., Horn, D. V., 2014. The McMurdo Dry Valleys: A landscape on the threshold of change. *Geomorphology*, 225(C), 25 – 35.

Luthcke, S. B., Brunt, K., 2023. ICESat-2 Project Science OfficeValidation and Calibration. *ICESat-2 Science Team Meeting*.

Luthcke, S. B., Thomas, T. C., Pennington, T. A., Rebold, T. W., Nicholas, J. B., Rowlands, D. D., Gardner, A. S., Bae, S., 2021. ICESat-2 Pointing Calibration and Geolocation Performance. *Earth and Space Science*, 8(3), e2020EA001494.

Magruder, L. A., Farrell, S. L., Neuenschwander, A., Duncanson, L., Csatho, B., Kacimi, S., Fricker, H. A., 2024. Monitoring Earth’s climate variables with satellite laser altimetry. *Nature Reviews Earth & Environment*, 1–17.

Markus, T., Neumann, T., Martino, A., Abdalati, W., Brunt, K., Csatho, B., Farrell, S., Fricker, H., Gardner, A., Harding, D., Jasinski, M., Kwok, R., Magruder, L., Lubin, D., Luthcke, S., Morison, J., Nelson, R., Neuenschwander, A., Palm, S., Popescu, S., Shum, C. K., Schutz, B. E., Smith, B., Yang, Y., Zwally, J., 2017. The Ice, Cloud, and land Elevation Satellite-2 (ICESat-2): Science requirements, concept, and implementation. *Remote Sensing of Environment*, 190, 260 – 273. http://dx.doi.org/10.1016/j.rse.2016.12.029.

Neumann, T. A., Martino, A. J., Markus, T., Bae, S., Bock, M. R., Brenner, A. C., Brunt, K. M., Cavanaugh, J., Fernandes, S. T., Hancock, D. W., Harbeck, K., Lee, J., Kurtz, N. T., Luers, P. J., Luthcke, S. B., Magruder, L., Pennington, T. A., Ramos-Izquierdo, L., Rebold, T., Skoog, J., Thomas, T. C., 2019. The Ice, Cloud, and Land Elevation Satellite – 2 mission_ A global geolocated photon product derived from the Advanced Topographic Laser Altimeter System. *Remote Sensing of Environment*, 233, 111325.

Schenk, T., Csatho, B., Neumann, T., 2022. Assessment of ICESat-2’s Horizontal Accuracy Using Precisely Surveyed Terrains in McMurdo Dry Valleys, Antarctica. *IEEE Transactions on Geoscience and Remote Sensing*, 60, 1–11.

Smith, B., Fricker, H. A., Holschuh, N., Gardner, A. S., Adusumilli, S., Brunt, K. M., Csatho, B., Harbeck, K., Huth, A., Neumann, T., Nilsson, J., Siegfried, M. R., 2019. Land ice height-retrieval algorithm for NASA’s ICESat-2 photon-counting laser altimeter. *Remote Sensing of Environment*, 233, 111352.

Zwally, H., Schutz, B., Abdalati, W., Abshire, J., Bentley, C., Brenner, A., Bufton, J., Dezio, J., Hancock, D., Harding, D., Herring, T., Minster, B., Quinn, K., Palm, S., Spinhirne, J., Thomas, R., 2002. ICESat’s laser measurements of polar ice, atmosphere, ocean, and land. *Journal of Geodynamics*, 34(3-4), 405–445.